

RSC Advances



This is an *Accepted Manuscript*, which has been through the Royal Society of Chemistry peer review process and has been accepted for publication.

Accepted Manuscripts are published online shortly after acceptance, before technical editing, formatting and proof reading. Using this free service, authors can make their results available to the community, in citable form, before we publish the edited article. This *Accepted Manuscript* will be replaced by the edited, formatted and paginated article as soon as this is available.

You can find more information about *Accepted Manuscripts* in the [Information for Authors](#).

Please note that technical editing may introduce minor changes to the text and/or graphics, which may alter content. The journal's standard [Terms & Conditions](#) and the [Ethical guidelines](#) still apply. In no event shall the Royal Society of Chemistry be held responsible for any errors or omissions in this *Accepted Manuscript* or any consequences arising from the use of any information it contains.

Performance of steel slag in carbonation–calcination looping for CO₂ capture from industrial flue gas

Si-cong Tian,^a Jian-guo Jiang,^{*a,b,c} Kai-min Li,^a Feng Yan^a and Xue-jing Chen^a

^aSchool of Environment, Tsinghua University, Beijing 100084, P. R. China. E-mail: jianguoj@mail.tsinghua.edu.cn; Tel: 86-10-62783548; Fax: 86-10-62783548.

^bKey Laboratory for Solid Waste Management and Environment Safety, Ministry of Education of China, P. R. China

^cCollaborative Innovation Center for Regional Environmental Quality, Tsinghua University, Beijing, P. R. China

Abstract: We investigate the performance of steel slag during the carbonation–calcination looping as a potential CO₂ adsorbent. The existence of portlandite in the steel slag provided a maximum theoretical CO₂ capture capacity of 112.7 mg_{CO₂} g_{slag}⁻¹, and the maximum carbonation conversion of 39.8% was achieved in simulated flue gases with only 5-min duration of carbonation. Sintering of the steel slag particles during both the carbonation and calcination processes, especially the destruction of the 3-nm pores, is the main cause for the deactivation of steel slag. Carbonation–calcination looping of steel slag can significantly improve its total CO₂ capture capacity compared to the conventional technical route of direct carbonation sequestration, thus providing an alternative and more feasible option for the use of alkaline industrial wastes to capture CO₂ from industrial sources, such as the iron and steel production facilities.

Anthropogenic CO₂ emissions are generally acknowledged to be the most important driving force of global climate change, and contribute about two-thirds of the enhanced greenhouse effect.¹ At present, about 32 billion tons of CO₂ are emitted into the atmosphere annually,² and almost 40% of worldwide CO₂ emissions are directly

attributable to industrial activities,³ such as iron and steel production, cement production, production of chemicals and petrochemicals, and the power generation sector due to electricity use in these industries.⁴ Reducing CO₂ emissions from these industrial sources is an essential part of the global response to prevent dangerous climate change. As the first generation and also a classical post-combustion capture technology for CO₂, amine scrubbing has been widely investigated and recently demonstrated on a pilot-scale.^{5,6} However, the problems of serious amine loss and the considerable energy consumption during the regeneration of absorbents, the weak vapor resistance in flue gas, and equipment corrosion, have significantly restricted the further development and application of this technology.^{7,8} Therefore, the use of solid-state adsorptive materials, such as a CaO-based adsorbent^{9,10}, zeolite^{11,12}, metal organic frameworks (MOF)¹³⁻¹⁵, and porous silica-supported amines hybrids¹⁶⁻¹⁸, became the focus of the development of the second-generation carbon capture and storage (CCS) technologies, due to their superior heat and mass transfer¹⁹, easier combination with existing industrialized facilities²⁰, and higher efficiency of energy utilization²¹. CaO-based adsorbents are one of the most promising of these solid adsorbents,²² when considering the cost of adsorbent synthesis, the resistance of impurities in flue gas, and the temperature experienced under actual application conditions (the temperature of flue gas is generally higher than 373 K).

The mineral carbonation sequestration of CO₂, which is also based on the carbonation reaction between CO₂ and certain alkaline calcium- or magnesium-rich minerals,²³ is another promising technique.²⁴ Natural minerals, such as wollastonite, serpentine and olivine, were initially considered as potential CO₂ sequestration materials, due to their huge potential capacity to sequester all of the CO₂ that might be emitted from the combustion of all the coal present on Earth.²⁵ However, the problems of the slow CO₂ sequestration rate, severe reaction conditions, and mineral mining or flue gas transportation, makes the CO₂ capture cost of this route uneconomic.^{26,27} Therefore, alkaline calcium-based industrial solid wastes, especially steel slag, have received more attention as alternative CO₂ sequestration materials,²⁸⁻³⁰ because they have the advantages of being readily available within the same industrial processes

where CO₂ is produced and have a better reaction activity with CO₂.³¹ Their use could reduce the cost of using industrial wastes for CO₂ sequestration by almost 30% compared to the use of natural minerals.³² However, the total CO₂ sequestration capacity of alkaline calcium-based industrial wastes is very limited, with the amount of steel slag produced globally permitting theoretically 44-59 Mt CO₂ per year. Due to the amount of available industrial wastes being much lower than the amount of available natural minerals, and being far below the global demand for CO₂ capture from industrial sources, the development of this technology is restricted.

Therefore, to improve the total CO₂ capture capacity of industrial wastes such as steel slag, we investigated the performance of steel slag as a potential CO₂ adsorbent during carbonation–calcination looping. The characteristics of the reaction kinetics and the deactivation mechanism for CaO-based adsorbents during the carbonation–calcination looping process were also analyzed.

The weight range curves in Fig. 1 clearly show the influence of temperature and CO₂ concentrations on the carbonation–decarbonation of steel slag. The steel slag sample almost had no capture effect on CO₂ in all reaction gases below 300 °C, but then begun to capture CO₂ with the sequestration rate accelerating gradually as the CO₂ concentration in the reaction atmosphere increased from 5% to 100%. The CO₂ sequestration rate remained at a high level as the temperature was continuously increased to 600 °C. When the heating continued, the steel slag abruptly decarbonated, and the maximum decarbonation rate was achieved at higher temperatures for gases with the higher CO₂ concentrations in the reaction atmosphere. The range of temperatures for the maximum decarbonation rate could be as large as 150 °C from 700 °C in a 5% CO₂ atmosphere to 850 °C in a 100% CO₂ atmosphere. This indicates that a temperature higher than 800 °C is required for steel slag to achieve the acceptable level of desorption for pure CO₂ to be further compressed and transported for permanent storage, since a purge gas with a higher CO₂ concentration is needed for the desorption process.

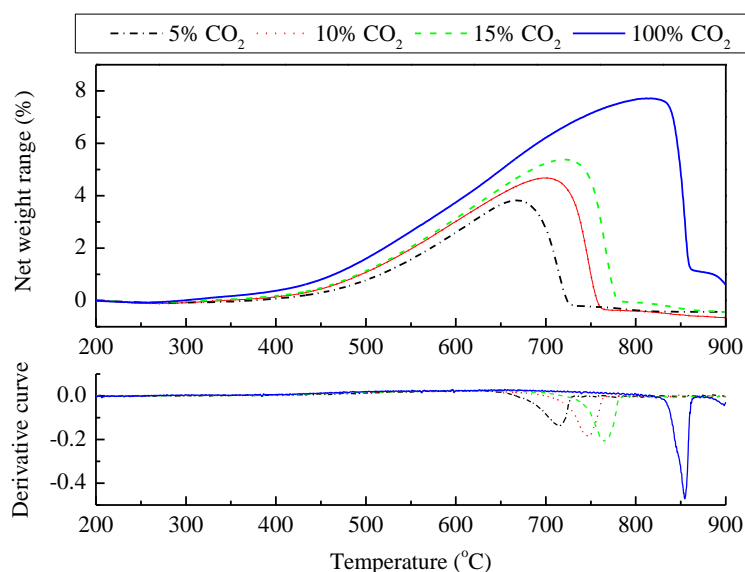


Fig. 1 Net CO₂ sequestration curve of steel slag at a heating rate of 10 °Cmin⁻¹ in different CO₂ concentrations.

Fig. 2 shows that although the steel slag achieved the same uptake of CO₂ from different reaction gases (see Table S1 in Electronic supplementary information) during the first carbonation–calcination looping, the CO₂ capture capacity of steel slag in a pure CO₂ atmosphere was clearly higher than in a 5–15% CO₂ atmosphere (i.e., the typical CO₂ concentrations in actual flue gas) during all the other cycles, and the cyclic capture of CO₂ by steel slag was equally efficient at CO₂ concentrations of 5–15%. This indicates that although CO₂ concentrations can influence the uptake of CO₂ by steel slag, there is almost no variation over the range of typical flue gas CO₂ concentrations.

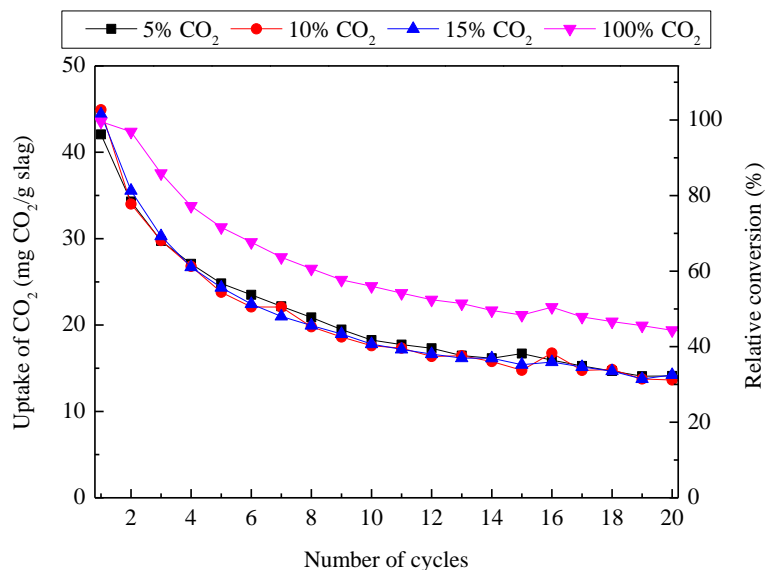


Fig. 2 CO₂ capture capacity of steel slag through 20 cycles in various CO₂ concentrations. The operating conditions were carbonation for 5 min at 600°C and calcination for 5 min at 800°C.

XRD patterns of the raw steel slag revealed the presence of Ca(OH)₂ in the sample, giving the steel slag a maximum theoretical CO₂ capture potential of 112.7 mgCO₂ g_{slag}⁻¹ (see Fig. S1 and Table S3 in Electronic supplementary information). This value is not very high because almost 63.86% of the total calcium content in the slag sample determined from an XRF analysis (see Table S2 in Electronic supplementary information) existed in other phases than Ca(OH)₂, and was not available for the capture of CO₂. The maximum practical uptake of CO₂ by the steel slag used in this experiment all occurred in the first cycle, and was 43.5 mgCO₂ g_{slag}⁻¹ in a 100% CO₂ atmosphere and 44.9 mgCO₂ g_{slag}⁻¹ in a 10% CO₂ atmosphere. The uptake of CO₂ then decreased gradually as the looping continued. The CO₂ capture capacity of steel slag decayed sharply during the first five cycles, but maintained almost half of the initial level of CO₂ capture after 10 cycles. The steel slag sample then had a much better durability (cyclic stability) for CO₂ capture until the 20th cycle, with the variation of CO₂ capture capacity ranging by only about 20%. The uptake of CO₂ by steel slag from simulated flue gases (5%–15% CO₂) decreased to 13.6–14.2 mgCO₂ g_{slag}⁻¹ at the end of 20 cycles, which was ~30–35% of its initial capacity. However, the total CO₂

capture capacity of the steel slag was improved by at least fivefold compared to the conventional technical route of direct carbonation sequestration, even if only 10 carbonation–calcination looping cycles were considered.

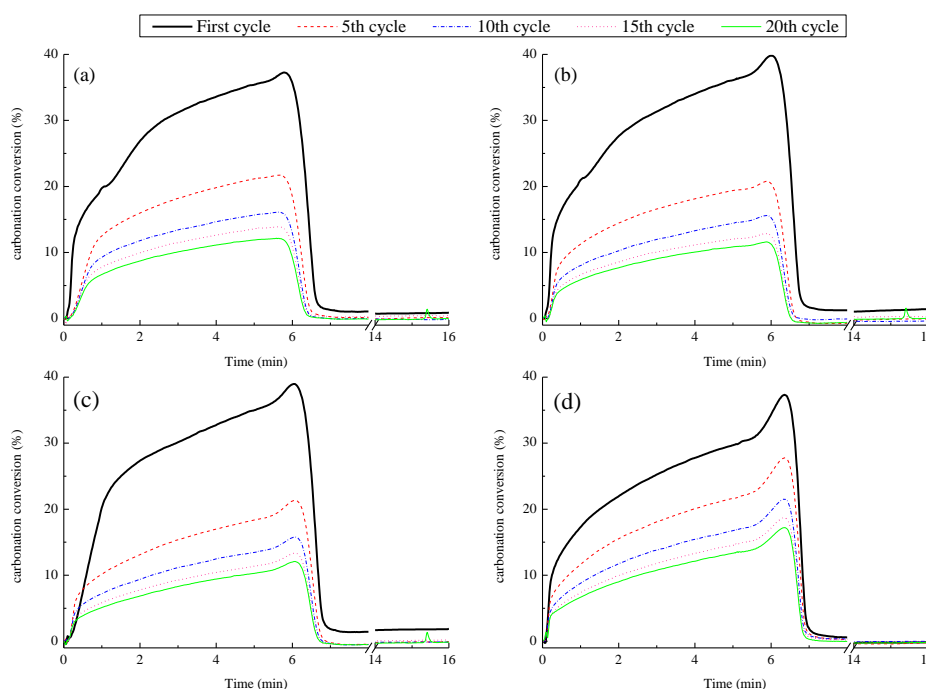


Fig. 3 Carbonation–decarbonation rates and the conversion of steel slag in simulated flue gases containing (a) 5% CO₂, (b) 10% CO₂, (c) 15% CO₂, and (d) 100% CO₂.

The CO₂ capture profiles of steel slag in the first, 5th, 10th, 15th, and 20th cycles (in Fig. 3) showed that in any individual looping cycle, the capture of CO₂ by steel slag occurred via a two-stage mechanism: a short but rapid stage, which was controlled by carbonation kinetics, followed by a long but slow stage, which was controlled by product layer diffusion. The carbonation rate of steel slag during the CO₂ adsorption process gradually reduced after multiple looping cycles in all reaction gases, and matched the decarbonation rate during the CO₂ desorption process. The carbonation of steel slag was still in the diffusion-controlled stage at the end of the CO₂ adsorption process, which was of 5-min duration, and the decarbonation rate was clearly faster than the carbonation rate in each looping cycle, with the adsorbed CO₂ abruptly released in a few tens of seconds. The carbonation conversion of the steel

slag used in this study ranged between 37.3% and 39.8% in the different simulated flue gases at the end of the initial looping cycle, which was slightly lower than that of the steel slag in other studies³³ and some other alkaline industrial wastes³⁴, which were used for the conventional carbonation sequestration of CO₂. This was a consequence of the much shorter reaction time (only 5-min duration for carbonation in this study) compared to direct carbonation sequestration. The carbonation conversion of the steel slag declined to about 16.1% after the 10th cycle, and finally 12.2% after the 20th cycle in the simulated flue gases.

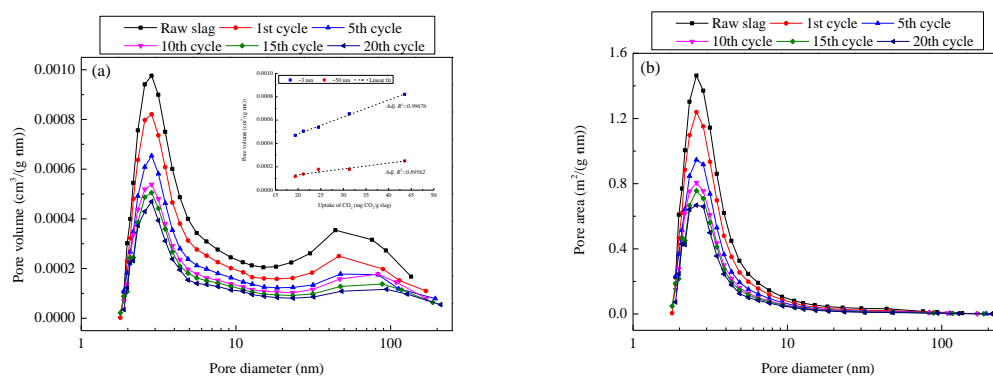


Fig. 4 Performance of the surface and pore properties of steel slag after multiple carbonation–calcination cycles in a pure CO₂ atmosphere: (a) Nitrogen physical adsorption of Barrett–Joyner–Halenda (BJH) dV/dD pore volume at 77 K, (b) Nitrogen physical adsorption of Barrett–Joyner–Halenda (BJH) dA/dD pore area at 77 K.

Surface and pore properties of the steel slag sample after multiple carbonation–calcination cycles in pure CO₂ are shown in Fig. 4. The Brunauer–Emmett–Teller (BET) surface area (see Fig. S3(a) in Electronic supplementary information) gradually decreased with the cyclic calcination in both air and a pure CO₂ atmosphere, and the steel slag that was calcined in a pure CO₂ atmosphere clearly had a lower BET surface area compared to the steel slag in air. This indicates that both the carbonation and calcination processes could cause a decay in the surface area of steel slag, which is typical for CaO-based CO₂ adsorbents. Furthermore, the carbonation process appeared to have a greater influence on the decay of the surface area than the

calcination process. The micro-pore area of the steel slag (see Fig. S3(b) in Electronic supplementary information) was not significantly influenced by the cyclic calcination in air after the 5th cycle, but decreased gradually in the presence of CO₂. This indicates that CO₂ could not only arrive at the meso-pores which largely existed in the steel slag sample, but also further diffuse into the micro-pores to react with the available Ca (CaO) in the steel slag particles. The formation of a bimodal pore-size distribution of the steel slag was observed after multiple carbonation–calcination cycles in Fig. 4(a), indicating that the smaller pores of ~3 nm and the larger pores of ~50 nm contributing most to the pore volume of the steel slag. Although pore volumes at both pore sizes had a significant decrease with the looping cycles, the 3-nm pores clearly had a stronger correlation with the CO₂ capture capacity of the steel slag than the 50-nm pores. This was probably because that the 3-nm pores could exactly provide the maximum surface area among all pore sizes of the steel slag (Fig. 4(b)), leaving relatively sufficient CaO active sites for the capture of CO₂. Therefore, sintering of the steel slag particles during both the carbonation and calcination processes, especially the destruction of the 3-nm pores, is the main cause for the decay of the CO₂ capture capacity of steel slag after multiple carbonation–calcination cycles. Besides sintering, an inadequate release of the adsorbed CO₂ during each carbonation–calcination looping cycle is another reason for the deactivation of steel slag, which can be clearly verified by the significant increase of the remaining CaCO₃ phase in the steel slag after multiple looping cycles (Fig. S4).

In summary, carbonation–calcination looping of steel slag for CO₂ capture from flue gas can significantly improve the CO₂ capture capacity of alkaline industrial wastes, such as steel slag, compared to the conventional route of direct carbonation sequestration, thus providing an alternative and more feasible option for the use of alkaline industrial wastes to *in situ* capture CO₂ from industrial sources. If the raw steel slag can be further restructured at the nano-micron scale to increase the content of the available CaO, it would become an ideal CO₂ adsorbent with the advantages of cost-savings, an abundant source and a high performance.

Acknowledgments

The authors gratefully acknowledge the Hi-Tech Research and Development Program (863) of China for financial support (Grant No. 2012AA06A116). The authors also acknowledge the support from Shanghai Tongji Gao Tingyao Environmental Science & Technology Development Foundation.

Notes and references

- 1 M. G. Nyambura, G. W. Mugeru, P. L. Felicia and N. P. Gathura, *J. Environ. Manage.*, 2011, **92**, 655.
- 2 World Bank WDI Database, <http://data.worldbank.org/indicator/EN.ATM.CO2E.KT/countries/1W?display=graph> and <http://data.worldbank.org/indicator/EN.ATM.CO2E.KT/countries/1W?display=default>.
- 3 International Energy Agency (IEA), Energy Technology Transitions for Industry, to be found under <http://www.iea.org/publications/freepublications/publication/industry2009.pdf>, pp. 30.
- 4 International Energy Agency (IEA), Tracking Clean Energy Progress 2013, to be found under http://www.iea.org/publications/freepublications/publication/TCEP_web.pdf, pp. 64-65.
- 5 J. Tollefson, *Nature*, 2011, **469**, 276.
- 6 M. A. Hussain, Y. Soujanya and G. N. Sastry, *Environ. Sci. Technol.*, 2011, **45**, 8582.
- 7 G. T. Rochelle, *Science*, 2009, **325**, 1652.
- 8 R. Steeneveldt, B. Berger and T. A. Torp, *Chem. Eng. Res. Des.*, 2006, **84**, 739.
- 9 V. Manovic and E. J. Anthony, *Environ. Sci. Technol.*, 2008, **42**, 4170.
- 10 F. N. Ridha, V. Manovic, A. Macchi and E. J. Anthony, *Int. J. Greenh. Gas Control*, 2012, **6**, 164.

- 11 M. Clause, J. Merel and F. Meunier, *Int. J. Greenh. Gas Control*, 2011, **5**, 1206.
- 12 F. S. Su and C. Y. Lu, *Energy Environ. Sci.*, 2012, **5**, 9021.
- 13 R. Banerjee, A. Phan, B. Wang, C. Knobler, H. Furukawa, M. O’Keeffe and O. M. Yaghi, *Science*, 2008, **319**, 939.
- 14 R. Vaidhyanathan, S. S. Iremonger, G. K. H. Shimizu, P. G. Boyd, S. Alavi and T. K. Woo, *Angew. Chem. Int. Ed.*, 2012, **51**, 1826.
- 15 Q. Y. Yang, S. Vaesen, F. Ragon, A. D. Wiersum, D. Wu, A. Lago, T. Devic, C. Martineau, F. Taulelle, P. L. Llewellyn, H. Jobic, C. L. Zhong, C. Serre, G. D. Weireld and G. Maurin, *Angew. Chem. Int. Ed.*, 2013, **52**, 10316.
- 16 A. Sayari and Y. Belmabkhout, *J. Am. Chem. Soc.*, 2010, **132**, 6312.
- 17 N. A. Brunelli, S. A. Didas, K. Venkatasubbiah and C. W. Jones, *J. Am. Chem. Soc.*, 2012, **134**, 13950.
- 18 P. S. Nugent, V. L. Rhodus, T. Pham, K. Forrest, L. Wojtas, B. Space and M. J. Zaworotko, *J. Am. Chem. Soc.*, 2013, **135**, 10950.
- 19 Q. Wang, J. Z. Luo, Z. Y. Zhong and A. Borgna, *Energy Environ. Sci.*, 2011, **4**, 42.
- 20 A. S. Bhowan and B. C. Freeman, *Environ. Sci. Technol.*, 2011, **45**, 8624.
- 21 M. L. Gray, K. J. Champagne, D. Fauth, J. P. Baltrus and H. Pennline, *Int. J. Greenhouse Gas Control*, 2008, **2**, 3.
- 22 M. Zhao, A. I. Minett and A. T. Harris, *Energy Environ. Sci.*, 2013, **6**, 25.
- 23 W. Seifritz, *Nature*, 1990, **345**, 486.
- 24 R. Zevenhoven, J. Fagerlund and J. K. Songok, *Greenhouse Gases*, 2011, **1**, 48.
- 25 P. B. Kelemen and J. Matter, *Proc. Natl. Acad. Sci. U. S. A.*, 2008, **105**, 17295.
- 26 M. M. Maroto-Valer, D. J. Fauth, M. E. Kuchta, Y. Zhang and J. M. Andresen, *Fuel Process. Technol.*, 2005, **86**, 1627.
- 27 S. J. Gerdemann, W. K. O’Connor, D. C. Dahlin, L. R. Penner and H. Rush, *Environ. Sci. Technol.*, 2007, **41**, 2587.
- 28 P. Renforth, C. L. Washbourne, J. Taylder and D. A. C. Manning, *Environ. Sci. Technol.*, 2011, **45**, 2035.
- 29 A. Sanna, M. Dri, M. R. Hall and M. Maroto-Valer, *Appl. Energy*, 2012, **99**, 545.
- 30 S. Y. Pan, E. E. Chang and P. C. Chiang, *Aerosol Air Qual. Res.*, 2012, **12**, 770.

- 31 P. J. Gunning, C. D. Hills and P. J. Carey, *Waste Manage.*, 2010, **30**, 1081.
- 32 W. J. J. Huijgen, R. N. J. Comans and G. J. Witkamp, *Energy Conv. Manag.*, 2007, **48**, 1923.
- 33 S. C. Tian, J. G. Jiang, X. J. Chen, F. Yan and K. M. Li, *ChemSusChem*, 2013, DOI: 10.1002/cssc.201300436.
- 34 S. C. Tian and J. G. Jiang, *Environ. Sci. Technol.*, 2012, **46**, 13545.

The English in this document has been checked by at least two professional editors, both native speakers of English. For a certificate, please see:

<http://www.textcheck.com/certificate/6EBSUB>